Mpemba effect of a mean-field system: The phase transition time

Zhen-Yu Yang[*] and Ji-Xuan Hou[†]
School of Physics, Southeast University, Nanjing 211189, China

(Received 26 July 2021; accepted 6 January 2022; published 19 January 2022)

The counterintuitive phenomenon—that an initially hotter water freezes faster than initially cooler water—is named the "Mpemba effect." Although it has been known for centuries, the underlying mechanism remains unclear. Recently, the Mpemba effect rekindled the interest of researchers since several studies identified that it might occur in some Markovian systems, and a general statistical-physical Mpemba effect framework was correspondingly proposed. In our previous study [Z.-Y. Yang and J.-X. Hou, Phys. Rev. E **101**, 052106 (2020)], we observed the non-Markovian Mpemba effect in a mean-field system (MFS), where the Mpemba effect originates from the back-reaction of the thermal reservoir. Naturally, the phase transition time is the key to the occurrence of the Mpemba effect, which, however, has not been quantitatively described. Following the direction of previous work, this study rigorously derives the phase transition time under different conditions, and quantitatively describes the mechanism of the non-Markovian Mpemba effect in a MFS. In addition, the validation of our theory was further verified via the microcanonical Monte Carlo simulation. An accurate description of the underlying mechanism of our proposed MFS facilitates the generalization of the Mpemba effect framework in statistical physics and may benefit in answering the riddle of the century, the original Mpemba effect in water.

DOI: 10.1103/PhysRevE.105.014119

I. INTRODUCTION

The Mpemba effect originally refers to the phenomenon that a beaker of initially hot water freezes faster than an initially cooler one. Although the earliest noted observation can be dated back to ancient times [1,2], the exact underlying mechanism of this counterintuitive phenomenon remains unclear [3–12]. Even its existence has been questioned after careful experimental analysis [13]. However, recent studies have found that the Mpemba effect may occur in several nonwater substances, which has again aroused interest in this field [14–23]. Subsequently, a general statistical-physical Mpemba effect framework has been proposed. The framework refers to the study of the phenomenon that two samples of the substance are in the same macroscopic state (except for their initial temperature), and the substance with the higher initial temperature quenches faster to the lower temperature. In this way, the Mpemba effect has been reported in many Markovian systems, such as nanotube resonators [24], spin glasses [25], granular fluids [26], and the Ising model [15]. However, the underlying mechanisms of the effect vary. For example, the Mpemba effect in granular fluids and spin glasses arises from additional factors controlling the temperature relaxation [25,26]. In the Ising model and the three-state system, the effect is caused by quenching along different trajectories for systems with different initial preparations [15].

Our previous study [27] observed the Mpemba effect in a non-Markovian system. Completely different from the Markovian process, the Mpemba effect in our model originates from the back-reaction of the thermal reservoir. Thus, it is the embodiment of the non-Markovianness in relaxation. Simply put, we investigated a mean-field system (MFS) placed in a staggered magnetic field. As the temperature of the MFS decreases, the system experiences the first-order phase transition from the paramagnetic state to the ferromagnetic state. Experimentally, when an MFS prepared to a high-temperature ferromagnetic state contacts with a huge cold thermal reservoir, the system will rapidly cool and then trap into a mid-temperature metastable ferromagnetic state. To evolve to the final low-temperature ferromagnetic state, the MFS needs to cross an energy barrier via thermal fluctuation. An initially hotter MFS has a stronger back-reaction to the thermal reservoir than an initially cooler one, which leads to a smaller energy barrier. As a result, an initially hotter MFS may spend less time in the metastable state and, correspondingly, spend less time to finish the phase transition. Our previous work successfully observed such a phenomenon but only employed an empirical formula—the Arrhenius law [28,29]—to estimate the metastable state lifetime. However, the formula becomes invalid when the size of the thermal reservoir continues to increase. Therefore, our previous work only revealed the phenomenon, but lacked a rigorous quantitative description. Another natural but unresolved question is whether the Mpemba effect will still occur when the reservoir becomes superlarge, where the back-reaction from the MFS becomes negligible. Collectively, the principle of the non-Markovian Mpemba effect in the MFS needs to be further investigated, and a more accurate description of the phase transition time needs to be provided.

In this work, we aim to quantitatively describe the underlying mechanism of the non-Markovian Mpemba effect in the MFS. Specifically, we rigorously derived the

[*]Also at Department of Radiation Oncology, Duke University Medical Center, Durham, North Carolina, USA.
[†]jxhou@seu.edu.cn

theoretical expression of metastable state lifetime based on the fundamental statistical theory. Moreover, the validation of our derivation was examined via microcanonical Monte Carlo simulation. This paper is structured into four sections. The first section gives the mean-field system model and derives its fundamental physical quantity; the second section investigates the cooling process of the MFS and demonstrates the emergence of the Mpemba effect in the MFS; the third section gives the theoretical expression of the phase transition time of the MFS, which is then verified by the Monte Carlo simulation; and the final section summarizes the finding of this study. Our proposed MFS is a confirmed model in which the Mpemba effect occurs in a non-Markovian process. An accurate description of the phase transition time helps in understanding its underlying mechanism and facilitates the generalization of the Mpemba effect framework in statistical physics.

II. THE MEAN-FIELD SYSTEM

We consider an MFS composed of N_{M} fermions placed in a staggered magnetic field. The Hamiltonian reads

$$H_{\mathrm{M}} = -\sum_{n=1}^{\frac{N}{2}} \frac{K}{2} S_n + \sum_{n=\frac{N}{2}+1}^{N} \frac{K}{2} S_n - \frac{J}{2N}\left(\sum_{n=1}^{N} S_n\right)^2, \quad (1)$$

where $S_n = \pm 1$. The first two terms on the right-hand side represent the interaction with a staggered magnetic field, and K is the intensity of the magnetic field. The last term denotes the long-range mean-field coupling [30].

The main thermodynamic properties of the proposed MFS, including its entropy, energy, temperature, and phase diagram, can be obtained analytically in the microcanonical ensemble. Specifically, let the N_{M}^{L-} and N_{M}^{R+} be the downward spins on the left side ($1 \leqslant n \leqslant N_{\mathrm{M}}/2$) and upward spins on the right side ($N_{\mathrm{M}}/2 + 1 \leqslant n \leqslant N_{\mathrm{M}}$) of the MFS, respectively. The compliance number and the magnetization of the MFS are $U_{\mathrm{M}} \equiv (N_{\mathrm{M}}^{R+} + N_{\mathrm{M}}^{L-})$ and $M_{\mathrm{M}} \equiv 2(N_{\mathrm{M}}^{R+} - N_{\mathrm{M}}^{L-})$, respectively. Therefore, the total number of the microstates reads

$$\Omega_{\mathrm{M}} = \binom{N_{\mathrm{M}}/2}{N_{\mathrm{M}}^{L-}} \binom{N_{\mathrm{M}}/2}{N_{\mathrm{M}}^{R+}}. \quad (2)$$

Denoting $u_{\mathrm{M}} = U_{\mathrm{M}}/N_{\mathrm{M}}$ and $m_{\mathrm{M}} = M_{\mathrm{M}}/N_{\mathrm{M}}$, we have the energy per spin and the entropy per spin as

$$\varepsilon_{\mathrm{M}} = \frac{E_{\mathrm{M}}}{N_{\mathrm{M}}} - \frac{K}{2} = K(u_{\mathrm{M}} - 1) - \frac{J}{2} m_{\mathrm{M}}^2, \quad (3)$$

and

$$\begin{aligned} s_{\mathrm{M}}(\varepsilon_{\mathrm{M}}, m_{\mathrm{M}}) &= \frac{1}{N_{\mathrm{M}}} \ln \Omega_{\mathrm{M}} \\ &= -\frac{1}{2}\left(u_{\mathrm{M}} + \frac{m_{\mathrm{M}}}{2}\right) \ln\left(u_{\mathrm{M}} + \frac{m_{\mathrm{M}}}{2}\right) \\ &\quad -\frac{1}{2}\left(1 - u_{\mathrm{M}} - \frac{m_{\mathrm{M}}}{2}\right) \ln\left(1 - u_{\mathrm{M}} - \frac{m_{\mathrm{M}}}{2}\right) \\ &\quad -\frac{1}{2}\left(u_{\mathrm{M}} - \frac{m_{\mathrm{M}}}{2}\right) \ln\left(u_{\mathrm{M}} - \frac{m_{\mathrm{M}}}{2}\right) \\ &\quad -\frac{1}{2}\left(1 - u_{\mathrm{M}} + \frac{m_{\mathrm{M}}}{2}\right) \ln\left(1 - u_{\mathrm{M}} + \frac{m_{\mathrm{M}}}{2}\right), \end{aligned} \quad (4)$$

respectively. Note that the constant $-K/2$ is added to Eq. (3) to shift the energy zero for the convenience of the following discussion. Finally, we have the temperature of the system as

$$T_{\mathrm{M}} = \frac{1}{\partial s_{\mathrm{M}}(\varepsilon_{\mathrm{M}})/\partial \varepsilon_{\mathrm{M}}}. \quad (5)$$

The behavior of the MFS varies with the choice of Hamiltonian parameters K and J [31–38]. In the context of the Mpemba effect, we set $\{K = -0.93,\ J = 1\}$ to observe the first-order phase transition. Figure 1(a) shows the entropy $s_{\mathrm{M}}(\varepsilon_{\mathrm{M}}, m_{\mathrm{M}})$ of the above setting, where blank regions are inaccessible to the MFS. Such inaccessibility makes it so that the magnetization of this system cannot vary within the interval $[-1, +1]$ for any given energy ε_{M}, and thus ergodicity is broken. The global maximum of $s_{\mathrm{M}}(\varepsilon_{\mathrm{M}})$ at any given energy corresponds to the equilibrium state, highlighted as black and gray solid lines. And the local maximum entropy values, marked as black and gray dashed lines, can be regarded as the possible metastable states. Moreover, the black and gray correspond to the paramagnetic and ferromagnetic states. As the ε_{M} decreases, the system evolves from the paramagnetic state ($m_{\mathrm{M}} = 0$, solid black line) to the ferromagnetic state ($m_{\mathrm{M}} \neq 0$, solid gray lines), through a first-order phase transition at $\varepsilon_{\mathrm{M}} = 0.122$. Figures 1(b) and 1(c) show the corresponding final entropy evolution (s_{M}-ε_{M}) path and caloric (T_{M}-ε_{M}) curve, respectively.

III. THE MPEMBA EFFECT

To investigate the cooling behavior of the MFS in detail, we employe the microcanonical Monte Carlo (MC) simulation [39]. Specifically, the coupling between a hot MFS and a huge low-temperature thermal reservoir is simulated. For simplicity, the noninteractive two-level thermal reservoir (TTR) is adopted in this study. We initialize the MFS as a spin chain with $N_{\mathrm{M}} = 50$, and the TTR is set as 20 times larger than MFS (i.e., $N_{\mathrm{R}} = \alpha N_{\mathrm{M}},\ \alpha = 20$). Without loss of generality, the energy of TTR is set to 0 K, and the energy splitting between the two states is set to be unity. According to Eq. (3), we can set the MFS to any temperature or energy by manipulating the spin-up and spin-down ratio. Here, for illustration purposes, the energy ε_{M} is initiated to its maximum value 0.475, and correspondingly $T_{\mathrm{M}} \to \infty$. The TTR is initially prepared to 0 K ($\varepsilon_{\mathrm{R,i}} = 0$), suggesting that all the spins stayed at the lowest energy state.

Figure 2(a) shows the microcanonical MC simulation schematic diagram. In the simulation, the thermal contact between the MFS and the TTR was achieved by an additional degree of freedom, named "demon." The demon was introduced to carry a small amount of energy ε_{D}. ε_{D} is initially set to zero and always stays non-negative. In each MC step, one spin from the MFS or TTR is randomly selected and flipped. If the energy change of the full system $\Delta E_{\mathrm{full}} < 0$, the movement is accepted, and ε_{D} is increased by $|\Delta E_{\mathrm{full}}|$. If $0 \leqslant \Delta E_{\mathrm{full}} \leqslant \varepsilon_{\mathrm{D}}$, the trial move is also accepted, and $\varepsilon_{\mathrm{D}} = \varepsilon_{\mathrm{D}} - |\Delta E_{\mathrm{full}}|$. Otherwise, the movement is rejected.

Figure 2(b) shows the simulated cooling path in the ε_{M}-m_{M} plane. The MFS's temperature from high to low is represented by the gradient of red (dark gray) to yellow (light gray). As shown, the path does not strictly follow the theoretical

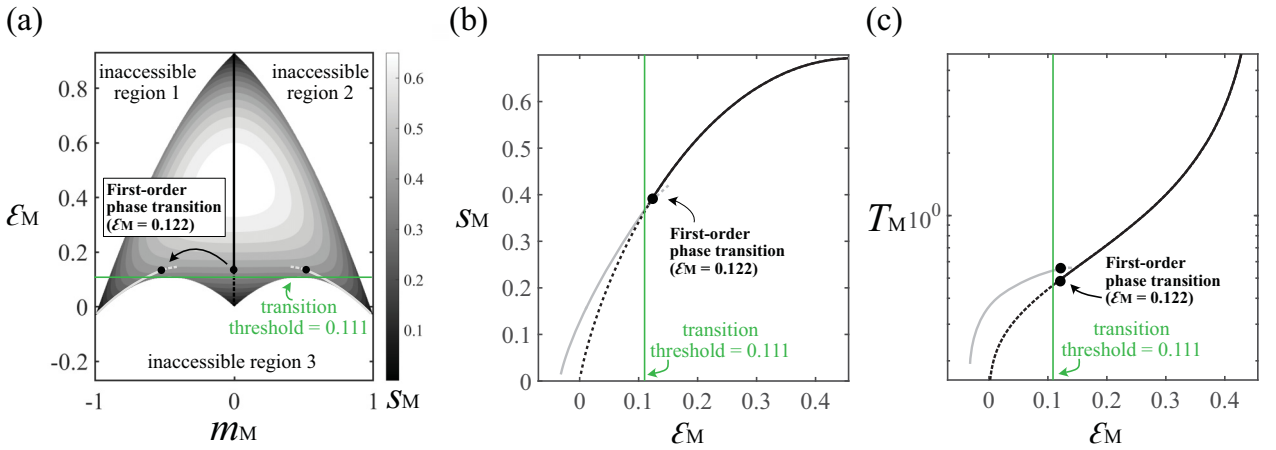

FIG. 1. Thermodynamic properties of the proposed mean-field system with $\{K = -0.93, J = 1\}$. (a) The entropy $s_M(\varepsilon_M, m_M)$ of the system, where the blank regions are inaccessible. The black and gray lines indicate the nonmagnetized and the ferromagnetic states, respectively. The solid lines are the global maximum of $s_M(\varepsilon_M)$ at any given energy (i.e., equilibrium state), while the dashed lines are the local maximum (i.e., possible metastable states). (b) The final entropy s_M of equilibrium and metastable states as a function of energy ε_M. (c) The corresponding caloric curve (T_M-ε_M).

equilibrium states in Fig. 1(a). Specifically, starting at the high-energy paramagnetic state (state I), the MFS first cools rapidly along the paramagnetic line. Due to the finiteness of the reservoir, the back-reaction from the MFS heats the reservoir during this process. Consequently, the MFS in the ferromagnetic state reaches a temporary equilibrium, i.e., the metastable state (state II), with the reservoir. It is useful to introduce an energy threshold ε_{th}, which corresponds to the topmost boundary of the inaccessible area 3 in Fig. 1(a). Here, $\varepsilon_{th} = 0.111$. Note that, for an isolated MFS in the metastable state with the energy $\varepsilon_M < \varepsilon_{th}$, it is impossible to spontaneously evolve from the paramagnetic state to the ferromagnetic state. However, for an MFS coupled with the thermal reservoir, the MFS can absorb additional energy $\Delta\varepsilon$ from the reservoir through thermal fluctuations within a certain time period, thereby getting across the threshold (state III) to the final equilibrium ferromagnetic state (state IV).

For a given finite cold thermal reservoir, the back-reaction of an initially hotter MFS heats it more than the initially cooler one. The free-energy barrier $\Delta\varepsilon$ is thus reduced, and less time will be spent in the metastable state. Suppose the total phase transition time τ depends primarily on the metastable state lifetime. In that case, an initially hot MFS can be quenched faster than the initially cooler one to the final ferromagnetic state. Consequently, the non-Markovian Mpemba effect can emerge. Figure 2(c) illustrates the time evolution of magnetization and energy of an initially hotter and an initially cooler MFS. Two independent MFSs are identical except for their initial temperature. The simulation configurations are were as above, that is, $N_M = 50$, $N_R = 20 \times 50$, and $\varepsilon_{R,i} = 0$.

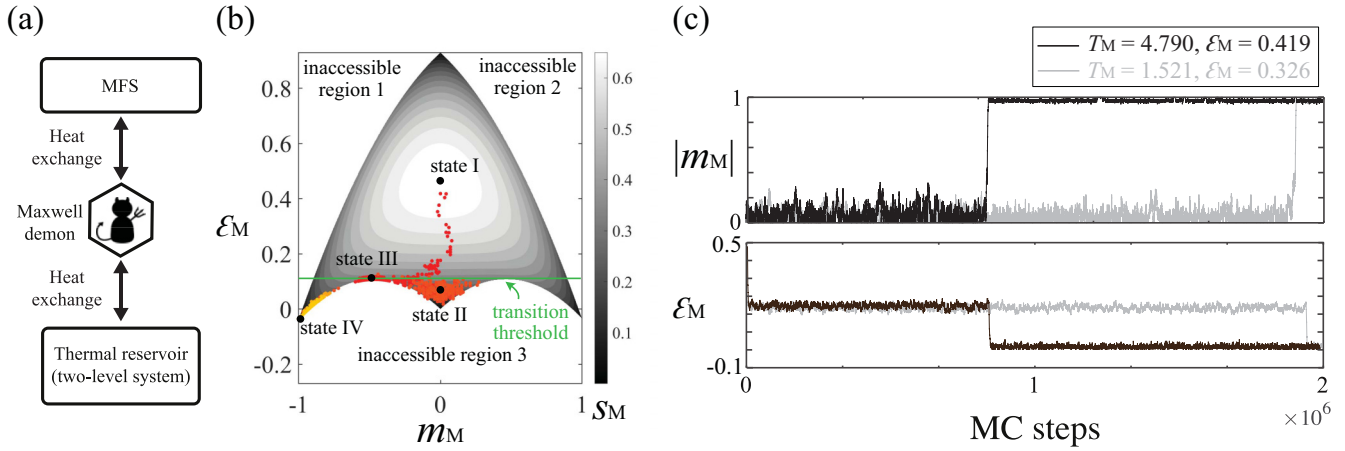

FIG. 2. (a) The microcanonical Monte Carlo simulation schematic diagram. (b) Time evolution path of an initially hot MFS coupled to a large cold reservoir. The MFS's temperature from high to low is represented by the gradient of red (dark gray) to yellow (light gray). Specifically, the MFS, initiated at a high-energy paramagnetic state (state I), first cools along the paramagnetic path to a metastable state (state II). After a certain period of time, the MFS absorbs additional energy via thermal fluctuations and gets across the threshold (state III) to the final equilibrium ferromagnetic state (state IV). (c) The emergence of the Mpemba effect in the MFS.

The black and gray lines represent the initially hotter and the initially cooler MFSs, which were initialized to $\{T_{\rm M} = 4.790, \varepsilon_{\rm M} = 0.419\}$ and $\{T_{\rm M} = 1.521, \varepsilon_{\rm M} = 0.326\}$, respectively. The sudden jump of $|m|$ declares the first-order phase transition from the paramagnetic to the ferromagnetic state. The abscissa MC steps are proportional to the time evolution [30,32]. Evidently, the Mpemba effect emerges in this experiment.

IV. TRANSITION TIME

The above experiments illustrate that the total phase transition time τ depends primarily on the metastable state lifetime of the MFS. However, the metastable state lifetime is affected by many factors, e.g., the initial temperature of the MFS, the size of the reservoir, etc. Naturally, for an MFS with a given initial temperature, a smaller reservoir will be heated to a higher temperature, corresponding to a smaller energy barrier and a faster phase transition. A fundamental theoretical derivation of phase transition time is desired to describe the phase transition of the MFS more accurately and comprehensively. Note that all the above derivation assumes that the total phase transition time τ is approximately equal to the lifetime of the MFS trapped in the metastable state.

For the TTR placed in an external magnetic field, its energy $\varepsilon_{\rm R}$ is equal to ± 1, as its spin can be the same as or the reverse of the direction of the magnetic field [40]. Let $N_{\rm R}$ represent the total spin of the TTR, and $N_{\rm R}^+$ and $N_{\rm R}^-$ be the downward and upward spins, respectively. Obviously, the total energy $E_{\rm R} = \varepsilon(N_{\rm R}^+ - N_{\rm R}^-)$. Easily, we have

$$N_{\rm R}^+ = \frac{N_{\rm R}}{2}\left(1 + \frac{E_{\rm R}}{N_{\rm R}\varepsilon_{\rm R}}\right), \quad N_{\rm R}^- = -\frac{N_{\rm R}}{2}\left(1 - \frac{E_{\rm R}}{N_{\rm R}\varepsilon_{\rm R}}\right). \tag{6}$$

Correspondingly, the entropy of the system is

$$S_{\rm R} = \ln \Omega_{\rm R} = \ln \frac{N_{\rm R}!}{N_{\rm R}^+! N_{\rm R}^-!}. \tag{7}$$

By shifting the energy zeros of the TTR to its energy minimum, the entropy per particle, $s_{\rm R}$, with respect to its energy $\varepsilon_{\rm R}$ is easily found as

$$s_{\rm R}(\varepsilon_{\rm R}) = \ln 2 - \tfrac{1}{2}\varepsilon_{\rm R} \ln \varepsilon_{\rm R} - \tfrac{1}{2}(2 - \varepsilon_{\rm R}) \ln (2 - \varepsilon_{\rm R}). \tag{8}$$

From Eq. (4), the entropy of the MFS in the paramagnetic ($m_{\rm M} = 0$) metastable state, $s_{\rm M,meta}$, is governed by

$$s_{\rm M,meta}(\varepsilon_{\rm M}) = -\left(1 + \frac{\varepsilon_{\rm M}}{K}\right) \ln \left(1 + \frac{\varepsilon_{\rm M}}{K}\right) + \frac{\varepsilon_{\rm M}}{K} \ln \left(-\frac{\varepsilon_{\rm M}}{K}\right). \tag{9}$$

The total energy of the full system, composed of the TTR and the MFS in the metastable state, is contributed by the initial energy of the MFS, $\varepsilon_{\rm M,i}$, only, i.e., $N_{\rm R}\varepsilon_{\rm R} + N_{\rm M}\varepsilon_{\rm M} = N_{\rm M}\varepsilon_{\rm M,i}$. Keeping the total energy constant, we express the total entropy of the full system, $S_{\rm full}$, as

$$S_{\rm full}(\varepsilon_{\rm M}, \varepsilon_{\rm R}) = N_{\rm M} s_{\rm M,meta}(\varepsilon_{\rm M}) + N_{\rm R} s_{\rm R}(\varepsilon_{\rm R}),$$

that is,

$$S_{\rm full}(\varepsilon_{\rm M}) = N_{\rm M} s_{\rm M,meta}(\varepsilon_{\rm M}) + N_{\rm R} s_{\rm R}\left[\frac{N_{\rm M}}{N_{\rm R}}(\varepsilon_{\rm M,i} - \varepsilon_{\rm M})\right]. \tag{10}$$

Based on the second law of thermodynamics, the metastable state of the MFS is located where the total entropy of the full system, $S_{\rm full}$, reaches its maximum. Here, $\varepsilon_{\rm M,i}$ is conserved and $\varepsilon_{\rm M}$ changes, so the energy of the MFS in the metastable state, $\varepsilon_{\rm M,meta}$, can be obtained by letting $\partial S_{\rm full}(\varepsilon_{\rm M})/\partial \varepsilon_{\rm M} = 0$. To get across the energy threshold $\varepsilon_{\rm th}$ and trigger the phase transition, the MFS needs to draw the energy with the amount of $\Delta\varepsilon = \varepsilon_{\rm th} - \varepsilon_{\rm M,meta}$ from the TTR, which leads to the entropy of the full system being decreased by $\Delta S_{\rm full} = S_{\rm full}(\varepsilon_{\rm M,meta}) - S_{\rm full}(\varepsilon_{\rm th})$. Finally, the transition time τ is governed by

$$\tau \sim \exp(\Delta S_{\rm full}). \tag{11}$$

Such exponential dependence on $N_{\rm M}$ has also been reported in the XY model [41] and gravitational systems [42].

A. The MFS coupling with a large TTR

Define $\alpha \equiv N_{\rm R}/N_{\rm M}$. If the MFS is coupled with a large TTR, e.g., $10 < \alpha < 30$, the first term on the right-hand side of Eq. (10) will be about ten times smaller than the second term, and thus it can be ignored. We have

$$S_{\rm full}(\varepsilon_{\rm M}) \approx N_{\rm R} S_{\rm R}\left[\frac{N_{\rm M}}{N_{\rm R}}(\varepsilon_{\rm M,i} - \varepsilon_{\rm M})\right]. \tag{12}$$

Then, $\Delta S_{\rm full}$ can be rewritten as

$$\frac{\Delta S_{\rm full}}{N_{\rm R}} \approx S_{\rm R}\left[\frac{N_{\rm M}}{N_{\rm R}}(\varepsilon_{\rm M,i} - \varepsilon_{\rm M,meta})\right] - S_{\rm R}\left[\frac{N_{\rm M}}{N_{\rm R}}(\varepsilon_{\rm M,i} - \varepsilon_{\rm th})\right]. \tag{13}$$

Based on our previous experiments [27], for the case where the MFS couples with a TTR that is only ten times larger, the back-reaction from the MFS will heat the reservoir to a relatively high temperature. Consequently, the temporary equilibrium between the MFS and the TTR is maintained at a high-energy state, leading to the energy of metastable state $\varepsilon_{\rm M,meta} \approx \varepsilon_{\rm th}$. Then we can perform the Taylor expansion on Eq. (13) and only keep its largest term,

$$\frac{\Delta S_{\rm full}}{N_{\rm R}} \approx \frac{N_{\rm M}}{N_{\rm R}} \frac{\partial s_{\rm R}}{\partial \varepsilon_{\rm R}}(\varepsilon_{\rm th} - \varepsilon_{\rm M,meta}),$$

that is, $\Delta S_{\rm full} \propto N_{\rm M}(\varepsilon_{\rm th} - \varepsilon_{\rm M,meta})$. Based on Eq. (11), we have

$$\tau \sim \exp[N_{\rm M}(\varepsilon_{\rm th} - \varepsilon_{\rm M,meta})] = \exp(N_{\rm M}\Delta\varepsilon), \tag{14}$$

where $\Delta\varepsilon$ is the amount of the energy barrier. Obviously, the initially hotter and larger MFS relaxes faster than the initially cooler and smaller MFS when coupled to a TTR that is only about ten times larger. Here, Eq. (14) coincides with the Arrhenius law. Such a law was utilized empirically in our previous work [27], where we set the TTR to be 15 times larger than the MFS. The above derivations prove the rationality of our previous adoption.

Note that the precise value of $\Delta\varepsilon$ can be obtained by calculating the exact location of the MFS's metastable state. Specifically, under the weak-coupling condition, the interaction energy between the MFS and the TTR is negligible, so the two subsystems remain isolated. And correspondingly, the energy of the full system equals the sum of the energies of two subsystems, i.e., $\varepsilon_{\rm full} = (\varepsilon_{\rm M,meta} + \alpha\varepsilon_{\rm R})/(1 + \alpha)$. The entropy per spin of the full system becomes $s_{\rm full}(\varepsilon_{\rm M,meta}, \varepsilon_{\rm R}) = (s_{\rm M,meta} + \alpha s_{\rm R})/(1 + \alpha)$. The $s_{\rm M,meta}$ has been obtained in Eq. (9). The equilibrium state is where the total entropy

reaches its maximum. Thus the entropy per spin of the full system is

$$s_{\text{full}}(\varepsilon_{\text{full}}) = \max_{\varepsilon_{\text{M,meta}}} s_{\text{full}}(\varepsilon_{\text{M,meta}}, \varepsilon_{\text{full}}) = \max_{\varepsilon_{\text{M,meta}}} \left(\frac{s_{\text{M,meta}} + \alpha s_{\text{R}}}{1+\alpha} \right). \quad (15)$$

By optimizing Eq. (15), each subsystem's energy, entropy, and temperature can be obtained. Thus, when giving the initial energy of the full system and the size of each subsystem, the exact amount of the energy barrier can be numerically derived.

B. The MFS coupling with a superlarge TTR

When the MFS is coupled with a superlarge TTR, e.g., $\alpha > 100$, the finite back-reaction from the MFS lets the energy allocated to each particle in the TTR become close to zero, i.e., $\varepsilon_{\text{R}} \approx 0$. Correspondingly, the temporary equilibrium between the MFS and the TTR is maintained at a very low-energy state. In this case, we can perform Taylor expansion on Eq. (8), and keep the leading term, so as to get

$$s_{\text{R}}(\varepsilon_{\text{R}}) \approx -\frac{\varepsilon_{\text{R}}}{2} \ln(\varepsilon_{\text{R}}). \quad (16)$$

Note that Eq. (12) and Eq. (13) still hold here. Substituting Eq. (16) into Eq. (13) and keeping the largest term, we have

$$\Delta S_{\text{full}} \approx -\frac{1}{2} N_{\text{M}} \varepsilon_{\text{th}} \ln \left[\frac{N_{\text{M}}}{N_{\text{R}}} (\varepsilon_{\text{M,i}} - \varepsilon_{\text{th}}) \right].$$

And finally, based on Eq. (11), we have

$$\ln \tau \sim \frac{1}{2} N_{\text{M}} \varepsilon_{\text{th}} \ln \left[\frac{N_{\text{R}}}{N_{\text{M}}} \frac{1}{\varepsilon_{\text{M,i}} - \varepsilon_{\text{th}}} \right] = \frac{1}{2} N_{\text{M}} \varepsilon_{\text{th}} \left[\ln \left(\frac{1}{\varepsilon_{\text{M,i}} - \varepsilon_{\text{th}}} \right) + \ln \alpha \right]. \quad (17)$$

Obviously, the result confirms that the transition time τ depends on both the initial energy or temperature of the MFS and the particle ratio α. Consequently, the Mpemba effect can still be observed when the reservoir becomes superlarge.

C. Monte Carlo simulation verification

The microcanonical MC simulation is again employed to examine the relationships in Eq. (14) and Eq. (17). The above theoretical calculations are all carried out under the thermodynamic limit. We also estimated the fit of the simulation with the theory under different particle numbers. If the number of particles is less than 30, there will be a great deviation from the theoretical value. Here we choose the number of particles to be 50. The same as the above experiment, we set $\varepsilon_{\text{R,i}} = 0$. The temperature and energy of the MFS was initiated to $\{T_{\text{M}} = 4.010, \varepsilon_{\text{M}} = 0.342\}$ or $\{T_{\text{M}} = 1.664, \varepsilon_{\text{M}} = 0.418\}$ to represent an initially hotter or initially cooler system, respectively.

Figure 3 shows the relationships between average transition time τ and ratio α in logarithmic scale, and the inset shows the first several points in Cartesian coordinates. The black circles and gray diamonds correspond to the experimental values of the initially hotter and initially cooler MFSs, respectively. The transition time, which refers to the Monte Carlo steps, was measured by 5000 independent MC simulations. The theoretical transition time obtained by Eq. (14) and Eq. (17) was shown in Fig. 3 with dashed lines and solid lines, respectively. Obviously, our theoretical framework agrees well with the experiment when $10 < \alpha < 30$ and $\alpha > 100$.

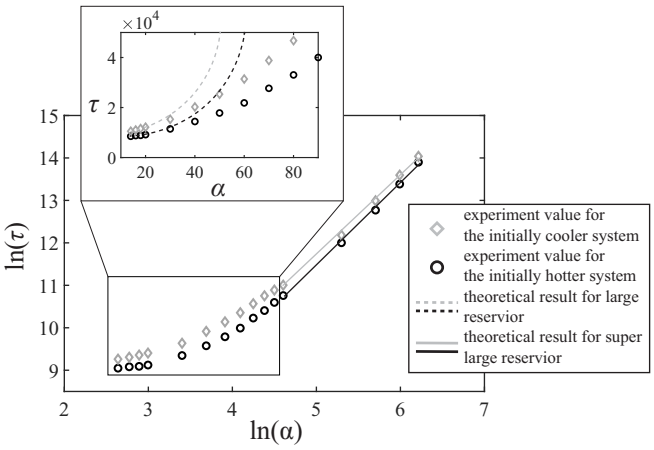

FIG. 3. The relationships between average transition time τ and ratio α in logarithmic scale. The inset shows the first several points in Cartesian coordinates. The black circles and gray diamonds correspond to experimental values of the initially hotter $\{T_{\text{M}} = 4.010, \varepsilon_{\text{M}} = 0.342\}$ and initially cooler $\{T_{\text{M}} = 1.664, \varepsilon_{\text{M}} = 0.418\}$ MFSs, respectively. The theoretical transition times obtained by Eq. (14) and Eq. (17) are shown with dashed lines and solid lines, respectively.

V. SUMMARY

The Mpemba effect has kept attracting researchers' interest for centuries. Our previous work [27] introduced the Mpemba effect into the non-Markovian process. This study is in line with the track of our previous work and describes the effect in more detail and more accurately. Naturally, the phase transition time τ is the key to eliciting the Mpemba effect. In this work, we derived the expressions of the phase transition time in detail for two cases: (1) when the MFS couples with a TTR that is only around ten times larger, τ depends both on the magnitude of the energy barrier and the number of the particles in the MFS; (2) when the MFS couples with a TTR that is more than 100 times larger, τ depends on the ratio of particle number in the TTR to the MFS. And the accurate mathematical expression of τ in both cases was given. Furthermore, the microcanonical Monte Carlo simulation verifies the above relationships. And the simulation results highly agree with our theoretical expressions.

Experimentally, our proposed MFS can be realized in a system constituted by a photon-mediated fermion gas arranged in a one-dimensional optical lattice by using the quantum-optical technique [43–46]. The simplicity of this model makes it an ideal prototype for studying the non-Markovian Mpemba effect in other, more complex, systems. And ultimately, the presented study may facilitate the generalization of the Mpemba-like effect framework and benefit in answering the riddle of the century, the original Mpemba effect in the water.

[1] M. Jeng, Am. J. Phys. **74**, 514 (2006).
[2] J. D. Brownridge, Am. J. Phys. **79**, 78 (2011).
[3] G. S. Kell, Am. J. Phys. **37**, 564 (1969).
[4] I. Firth, Phys. Educ. **6**, 32 (1971).
[5] M. Vynnycky, S. L. Mitchell, and N. Maeno, Heat Mass Transf. **47**, 863 (2011).
[6] E. Deeson, Phys. Educ. **6**, 42 (1971).
[7] R. T. Ibekwe and J. P. Cullerne, Phys. Educ. **51**, 025011 (2016).
[8] P. K. Maciejewski, J. Heat Transf. **118**, 65 (1996).
[9] M. Freeman, Phys. Educ. **14**, 417 (1979).
[10] J. I. Katz, Am. J. Phys. **77**, 27 (2009).
[11] B. Wojciechowski, I. Owczarek, and G. Bednarz, Cryst. Res. Technol. **23**, 843 (1988).
[12] X. Zhang, Y. Huang, Z. Ma, Y. Zhou, J. Zhou, W. Zheng, Q. Jiang, and C. Q. Sun, Phys. Chem. Chem. Phys. **16**, 22995 (2014).
[13] H. C. Burridge and P. F. Linden, Sci. Rep. **6**, 37665 (2016).
[14] Z. Lu and O. Raz, Proc. Natl. Acad. Sci. USA **114**, 5083 (2017).
[15] I. Klich, O. Raz, O. Hirschberg, and M. Vucelja, Phys. Rev. X **9**, 021060 (2019).
[16] A. Gal and O. Raz, Phys. Rev. Lett. **124**, 060602 (2020).
[17] J. Bechhoefer, A. Kumar, and R. Chétrite, Nat. Rev. Phys. **3**, 534 (2021).
[18] R. Chétrite, A. Kumar, and J. Bechhoefer, Front. Phys. (Beijing) **9**, 141 (2021).
[19] A. Kumar and J. Bechhoefer, Nature (London) **584**, 64 (2020).
[20] A. Torrente, M. A. López-Castaño, A. Lasanta, F. V. Reyes, A. Prados, and A. Santos, Phys. Rev. E **99**, 060901(R) (2019).
[21] E. Mompó, M. López-Castaño, A. Lasanta, F. Vega Reyes, and A. Torrente, Phys. Fluids **33**, 062005 (2021).
[22] F. Carollo, A. Lasanta, and I. Lesanovsky, Phys. Rev. Lett. **127**, 060401 (2021).
[23] N. Vadakkayil and S. K. Das, Phys. Chem. Chem. Phys. **23**, 11186 (2021).
[24] P. A. Greaney, G. Lani, G. Cicero, and J. C. Grossman, Metall. Mater. Trans. A **42**, 3907 (2011).
[25] M. Baity-Jesi, E. Calore, A. Cruz, L. A. Fernandez, J. M. Gil-Narvión, A. Gordillo-Guerrero, D. Iñiguez, A. Lasanta, A. Maiorano, E. Marinari *et al.*, Proc. Natl. Acad. Sci. USA **116**, 15350 (2019).
[26] A. Lasanta, F. Vega Reyes, A. Prados, and A. Santos, Phys. Rev. Lett. **119**, 148001 (2017).
[27] Z.-Y. Yang and J.-X. Hou, Phys. Rev. E **101**, 052106 (2020).
[28] L. Pauling, Soil Sci. **77**, 77 (1954).
[29] K. J. Laidler, *Chemical Kinetics* (Pearson India, 1987).
[30] D. Mukamel, S. Ruffo, and N. Schreiber, Phys. Rev. Lett. **95**, 240604 (2005).
[31] J.-X. Hou, X.-C. Yu, and J.-M. Hou, Int. J. Theor Phys. **55**, 3923 (2016).
[32] J.-X. Hou, Phys. Rev. E **99**, 052114 (2019).
[33] Z.-Y. Yang and J.-X. Hou, Eur. Phys. J. B **92**, 170 (2019).
[34] Z.-Y. Yang and J.-X. Hou, Mod. Phys. Lett. B **33**, 1950072 (2019).
[35] J.-X. Hou, Eur. Phys. J. B **93**, 82 (2020).
[36] J.-X. Hou, Eur. Phys. J. B **94**, 151 (2021).
[37] J.-X. Hou, Eur. Phys. J. B **94**, 6 (2021).
[38] J.-X. Hou, Phys. Rev. E **104**, 024114 (2021).
[39] M. Creutz, Phys. Rev. Lett. **69**, 1002 (1992).
[40] S. Salinas, *Introduction to Statistical Physics* (Springer Science & Business Media, New York, 2001).
[41] M. Antoni, S. Ruffo, and A. Torcini, Europhys. Lett. **66**, 645 (2004).
[42] P. H. Chavanis and M. Rieutord, Astron. Astrophys. **412**, 1 (2003).
[43] A. Griesmaier, J. Werner, S. Hensler, J. Stuhler, and T. Pfau, Phys. Rev. Lett. **94**, 160401 (2005).
[44] T. Graß and M. Lewenstein, EPJ Quantum Technol. **1**, 8 (2014).
[45] J. W. Britton, B. C. Sawyer, A. C. Keith, C.-C. J. Wang, J. K. Freericks, H. Uys, M. J. Biercuk, and J. J. Bollinger, Nature (London) **484**, 489 (2012).
[46] A. Micheli, G. Brennen, and P. Zoller, Nat. Phys. **2**, 341 (2006).